Diagrammatic Design of Ansätze for Quantum Chemistry

Ayman El Amrani

St. John's College

A thesis submitted for the Honour School of Chemistry

Part II 2024

Pour ma mère et mon père.

Acknowledgements

Thank you Thomas Cervoni for your constant motivation and support.

Thank you David Tew and Stefano Gogioso for your patient supervision.

Thank you Razin Shaikh, Boldizsár Poór, Richie Yeung and Harny Wang for always finding the time to answer my questions.

Thank you to my friends and family for supporting me during this unconvential Master's.

Summary

A central challenge in computational quantum chemistry is the accurate simulation of fermionic systems. At the heart of these calculations lies the need to solve the Schrödinger equation to determine the many-electron wavefunction. An exact solution to this problem scales exponentially with the number of electrons. Classical computers struggle to store the increasingly large wavefunctions making this problem computationally intractable in many cases. In contrast, gate-based quantum computing presents a promising solution, offering the potential to represent electronic wavefunctions with polynomially scaling resources [1]. In other words, quantum computers are a natural tool of choice for simulating processes that are inherently quantum [2].

In the last two decades many advancements in quantum computing have been made in both hardware and software bringing us closer to being able to simulate molecular systems. Despite these advancements, we remain in the so-called Noisy Intermediate Scale Quantum (NISQ) era, characterised by challenges such as poor qubit fidelity, low qubit connectivity and limited coherence times. The NISQ era represents a transitional phase in quantum computing, where quantum devices are not yet error-corrected but are still capable of performing computations beyond the reach of classical computers. Overcoming the limitations of the NISQ era is crucial for realising the full potential of quantum computing in various fields, including quantum chemistry and materials science.

The Variational Quantum Eigensolver (VQE) algorithm is a method used to estimate the ground state energy of a molecular Hamiltonian by preparing a trial wavefunction,

calculating its energy, and optimising the wavefunction parameters classically until the energy converges to the best approximation for the ground state energy [3]. It is recognised as a leading algorithm for quantum simulation on NISQ devices due to its reduced resource requirements in terms of qubit count and coherence time [4].

This thesis extends methods developed by Richie Yeung [2] for the preparation and analysis of parametrised quantum circuits, and applies them to ansätze representing fermionic wavefunctions. We are concerned with two main questions on this theme. Firstly, can we use the ZX calculus [cite] to gain insights into the structure of the unitary product ansatz in the context of variational algorithms for quantum chemistry? Secondly, in the context of NISQ devices, can we use these insights to build better ansätze with reduced circuit depth and more efficient resources?

Contents

Chapter 1

ZX Calculus

The ZX calculus is a diagrammatic language for reasoning about quantum processes that has seen a large increase in applications over the past 10 years. It provides a novel perspective on quantum computation and quantum mechanics.

1.1 Generators

By sequentially or horizontally composing the *Z Spider* (green) and *X Spider* (red) generators, we can construct undirected multigraphs known as ZX diagrams [5]. That is, graphs that allow multiple edges between vertices. Since *only connectivity matters* in the ZX calculus, a valid ZX diagram can be deformed as seen fit, provided that the order of inputs and outputs is preserved.

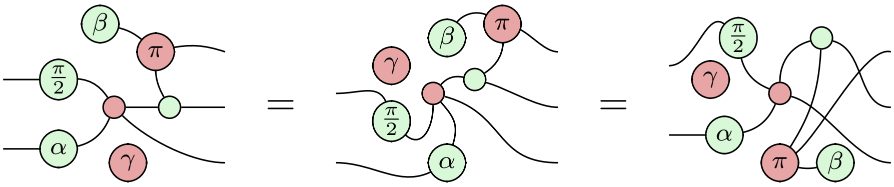

Figure 1.1: Three equivalent ZX diagrams (*only connectivity matters*).

Z Spiders are defined with respect to the Z eigenbasis such that a Z Spider with n inputs and m outputs has the following interpretation as a linear map. Note that in this text, we will interpret the flow of time from left to right.

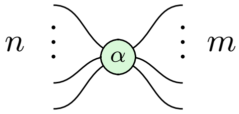

$$= |0\rangle^{\otimes m} \langle 0|^{\otimes n} + e^{i\alpha} |1\rangle^{\otimes m} \langle 1|^{\otimes n}$$

Figure 1.2: Interpretation of Z Spider as a linear map.

Similarly, X Spiders, which are defined with respect to the X eigenbasis, are interpreted as the following linear map.

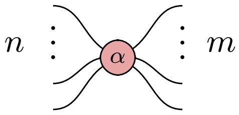

$$= |+\rangle^{\otimes m} \langle +|^{\otimes n} + e^{i\alpha} |-\rangle^{\otimes m} \langle -|^{\otimes n}$$

Figure 1.3: Interpretation of X Spider as a linear map.

We can recover the $|0\rangle$ eigenstate using an X Spider that has a phase of zero, or the $|1\rangle$ eigenstate using an X Spider that has a phase of π.

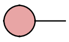

$$= |+\rangle + |-\rangle = \sqrt{2}\,|0\rangle$$

Figure 1.4: $|0\rangle$ eigenstate

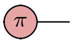

$$= |+\rangle - |-\rangle = \sqrt{2}\,|1\rangle$$

Figure 1.5: $|1\rangle$ eigenstate

Likewise, we have the $|+\rangle$ and $|-\rangle$ basis states from the corresponding Z Spider

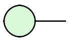

$$= |0\rangle + |1\rangle = \sqrt{2}\,|+\rangle$$

Figure 1.6: $|+\rangle$ eigenstate

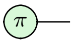

$$= |0\rangle - |1\rangle = \sqrt{2}\,|-\rangle$$

Figure 1.7: $|-\rangle$ eigenstate

Whilst we obtain the correct states, we obtain the wrong scalar factor. For the remainder of this thesis, we will ignore global non-zero scalar factors. Hence, equal signs should be interpreted as 'equal up to a global phase'.

Single qubit rotations in the Z basis are represented by a Z Spider with a single input and a single output. Arbitrary rotations in the X basis are represented by the corresponding X spider. We can view these as rotations of the Bloch sphere.

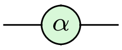

$$|0\rangle\langle 0| + e^{i\alpha}|1\rangle\langle 1| = \begin{pmatrix} 1 & 0 \\ 0 & e^{i\alpha} \end{pmatrix} \rightarrow$$

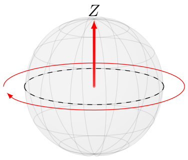

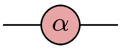

$$|+\rangle\langle +| + e^{i\alpha}|-\rangle\langle -| = \frac{1}{2}\begin{pmatrix} 1+e^{i\alpha} & 1-e^{i\alpha} \\ 1-e^{i\alpha} & 1+e^{i\alpha} \end{pmatrix} \rightarrow$$

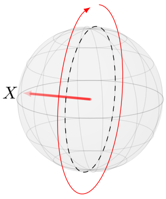

Figure 1.8: Arbitrary single qubit rotations in the Z and X bases.

We can recover the Pauli Z and Pauli X matrices by setting the angle $\alpha = \pi$.

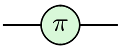

$$= |0\rangle\langle 0| + e^{i\pi}|1\rangle\langle 1| = \begin{pmatrix} 1 & 0 \\ 0 & -1 \end{pmatrix}$$

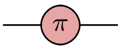

$$= |+\rangle\langle +| + e^{i\pi}|-\rangle\langle -| = \begin{pmatrix} 0 & 1 \\ 1 & 0 \end{pmatrix}$$

Figure 1.9: Pauli Z and X gates in the ZX calculus.

Composition

To calculate the matrix of a ZX diagram consisting of sequentially composed spiders, we take the matrix product. Note that the order of operation of matrix multiplication is the reverse as in the ZX diagram as we have defined it.

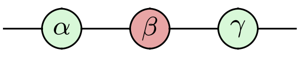

$$= \begin{pmatrix} 1 & 0 \\ 0 & e^{i\gamma} \end{pmatrix} \begin{pmatrix} 1+e^{i\beta} & 1-e^{i\beta} \\ 1-e^{i\beta} & 1+e^{i\beta} \end{pmatrix} \begin{pmatrix} 1 & 0 \\ 0 & e^{i\alpha} \end{pmatrix}$$

Alternatively, we could have chosen to compose the spiders in parallel, resulting in the tensor product.

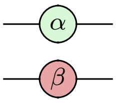

$$= \begin{pmatrix} 1 & 0 \\ 0 & e^{i\alpha} \end{pmatrix} \otimes \begin{pmatrix} 1+e^{i\beta} & 1-e^{i\beta} \\ 1-e^{i\beta} & 1+e^{i\beta} \end{pmatrix}$$

The CNOT gate in the ZX calculus is represented by a Z spider (control qubit) and an X spider (target qubit). We can arbitrarily deform the diagram and decompose it into matrix and tensor products as follows.

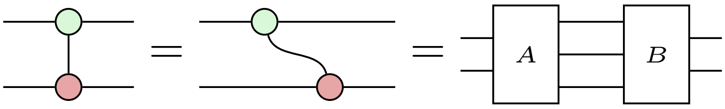

We can calculate matrix A, consisting of a single-input and two-output Z Spider (4×2 matrix) and an empty wire (identity matrix), by taking the tensor product.

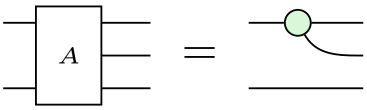

$$= \begin{pmatrix} 1 & 0 \\ 0 & 0 \\ 0 & 0 \\ 0 & 1 \end{pmatrix} \otimes \begin{pmatrix} 1 & 0 \\ 0 & 1 \end{pmatrix}$$

Similarly, to calculate the matrix B, we take the following tensor product.

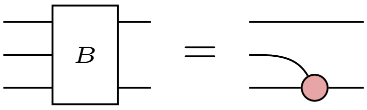

$$= \begin{pmatrix} 1 & 0 \\ 0 & 1 \end{pmatrix} \otimes \frac{1}{\sqrt{2}} \begin{pmatrix} 1 & 0 & 0 & 1 \\ 0 & 1 & 1 & 0 \end{pmatrix}$$

We can then calculate the CNOT matrix by taking the matrix product of matrix A and matrix B as follows.

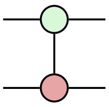

$$= \left[\begin{pmatrix} 1 & 0 \\ 0 & 1 \end{pmatrix} \otimes \frac{1}{\sqrt{2}} \begin{pmatrix} 1 & 0 & 0 & 1 \\ 0 & 1 & 1 & 0 \end{pmatrix} \right] \left[\begin{pmatrix} 1 & 0 \\ 0 & 0 \\ 0 & 0 \\ 0 & 1 \end{pmatrix} \otimes \begin{pmatrix} 1 & 0 \\ 0 & 1 \end{pmatrix} \right] \simeq \begin{pmatrix} 1 & 0 & 0 & 0 \\ 0 & 1 & 0 & 0 \\ 0 & 0 & 0 & 1 \\ 0 & 0 & 1 & 0 \end{pmatrix}$$

Had we chosen to make the first qubit the target and the second qubit the control, we would have obtained the following.

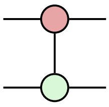

$$= \left[\frac{1}{\sqrt{2}}\begin{pmatrix}1&0&0&1\\0&1&1&0\end{pmatrix}\otimes\begin{pmatrix}1&0\\0&1\end{pmatrix}\right]\left[\begin{pmatrix}1&0\\0&1\end{pmatrix}\otimes\begin{pmatrix}1&0\\0&0\\0&0\\0&1\end{pmatrix}\right]\simeq\begin{pmatrix}1&0&0&0\\0&1&0&0\\0&0&0&1\\0&0&1&0\end{pmatrix}$$

Since *only connectivity matters*, we could have equivalently calculated the matrix of the CNOT gate by deforming the diagram as follows.

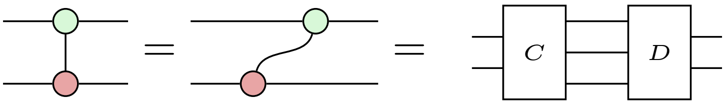

Hadamard Generator

All quantum gates are unitary transformations. Therefore, up to a global phase, an arbitrary single qubit rotation U can be viewed as a rotation of the Bloch sphere about some axis. We can decompose the unitary U using Euler angles to represent the rotation as three successive rotations [5].

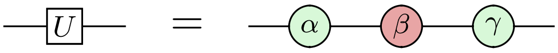

Figure 1.10: Arbitrary single-qubit rotation.

Recall that the Hadamard gate H switches between the $|0\rangle/|1\rangle$ and $|+\rangle/|-\rangle$ bases. That is, it corresponds to a rotation of the Bloch sphere π radians about the line bisecting the Z and X axes. By choosing $\alpha = \beta = \gamma = \frac{\pi}{2}$, we obtain the Hadamard gate up to a global phase of $e^{-i\frac{\pi}{4}}$. We define the Hadamard generator below.

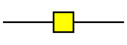

$$= e^{-i\frac{\pi}{4}}$$

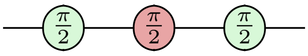

$$= \frac{1}{\sqrt{2}}\begin{pmatrix}1&1\\1&-1\end{pmatrix}$$

Figure 1.11: Hadamard generator in the ZX calculus.

There are many equivalent ways of decomposing the Hadamard gate using Euler angles. Note that the rightmost representations need no scalar corrections.

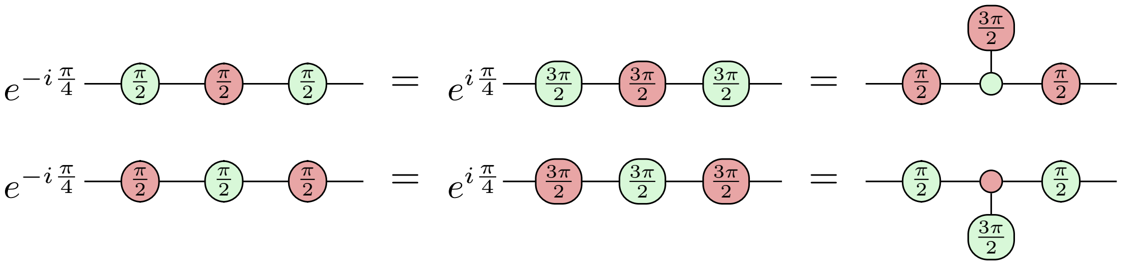

Figure 1.12: Equivalent definitions of the Hadamard generator.

Conjugate, Transpose and Adjoint

We can find the transpose of a ZX diagram by turning all of its inputs into outputs and all of its outputs into inputs whilst preserving the order of their wires.

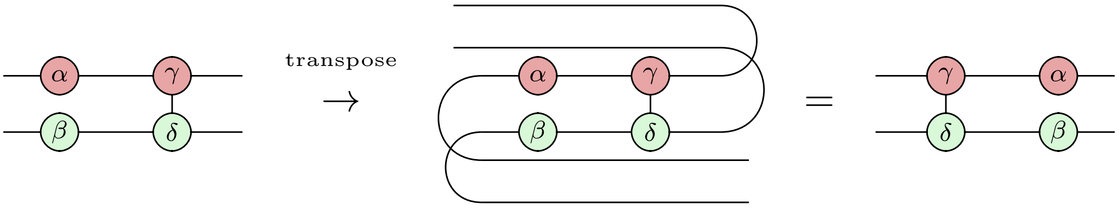

We can find the conjugate of a ZX diagram by simply negating the phases of all spiders in the diagram, $\alpha \to -\alpha,\ \beta \to -\beta, \ldots$.

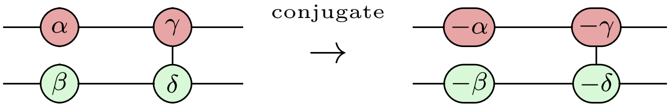

It is then a simple matter to find the Hermitian adjoint of a ZX diagram by first finding its conjugate, then its transpose.

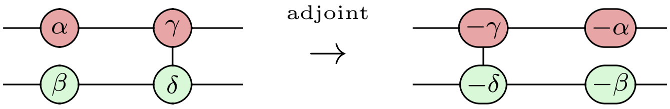

1.2 Rewrite Rules

This section introduces the various rewrite rules that come equipped with the ZX calculus. These rules extend the ZX calculus from notation into a language.

Spider Fusion

The most fundamental rule of the ZX calculus is the *spider fusion* rule [5]. It states that two spiders connected by one or more wires fuse if they are the same colour. It is the generalisation of adding the phases of successive rotations of the Bloch sphere. Since we interpret the phases α and β as $e^{i\alpha}$ and $e^{i\beta}$, it follows that the phase $\alpha + \beta$ is modulo 2π.

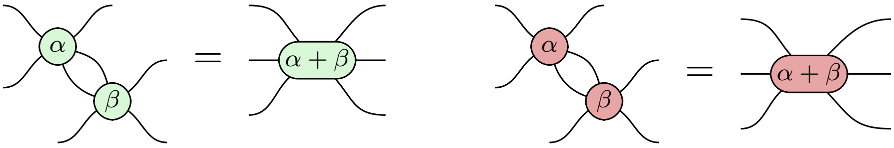

Figure 1.13: Spider fusion rule for Z spiders (left) and X spiders (right).

We can use this rule to identify commutation relations. For instance, Z rotations commute through CNOT controls and X rotations commute through CNOT targets.

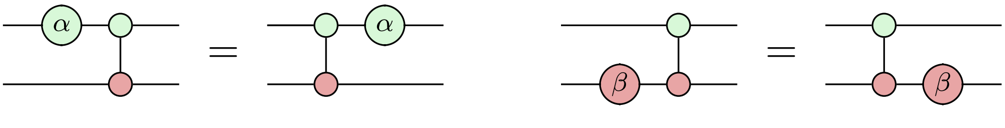

Identity Removal

The *identity removal* rule states that any two-legged spider with no phase ($\alpha = 0$) is equivalent to an empty wire since a rotation by 0 radians is the same as no rotation.

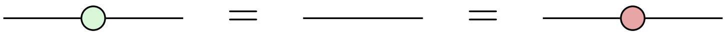

Figure 1.14: Identity removal rule.

Combining this with the spider fusion rule (1.2), we see that two successive rotations with opposite phases is equivalent to an empty wire.

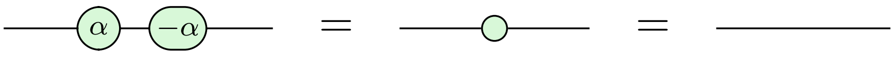

π Copy Rule

The π *copy* rule concerns itself with the interactions of the Pauli Z and X gates with spiders. It states that when a Pauli Z or Pauli X gate is pushed through a spider of the opposite colour, it copies through the spider and flips its phase.

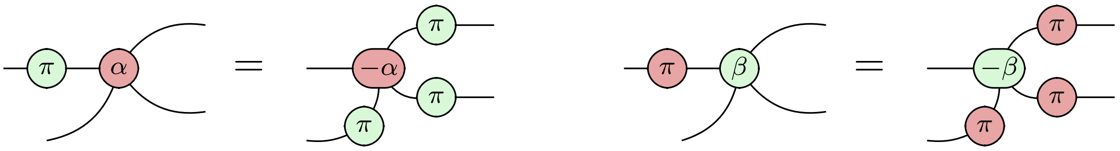

Figure 1.15: π copy rule for Z and and X spiders.

State Copy Rule

A similar rule derived from the π copy rule (1.2), is the *state copy* rule. It states that the $|0\rangle$ state (phaseless X spider) and the $|1\rangle$ state (X spider with phase π) interact with Z spiders as follows. The same rule holds for the colour-flipped counterparts.

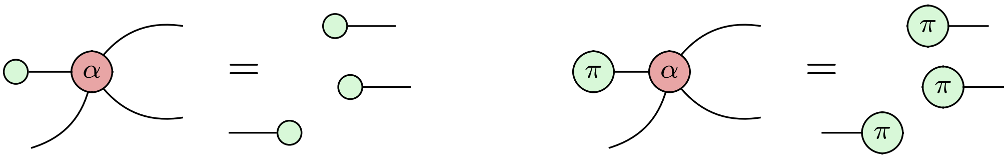

Figure 1.16: State copy rule for the X eigenstates.

Bialgebra Rule

Unlike the previous rules we have introduced, the *bialgebra rule* takes some time to understand intuitively. It is nethertheless important in many derivations. We can represent the eigenstates of the X and Z operators by introducing the boolean variable $a \in \{0, 1\}$ as follows.

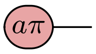 $= |0\rangle$ where $a = 0$ and $|1\rangle$ where $a = 1$

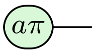 $= |+\rangle$ where $a = 0$ and $|-\rangle$ where $a = 1$

Using the spider fusion rule (1.2), we are able to show that an X spider with two inputs and one output behaves like the classical XOR gate when applied to the $|0\rangle$ and $|1\rangle$ states. Using the state copy rule (1.2), we are able to show that a Z spider with one input and two outputs behaves like the classical COPY gate.

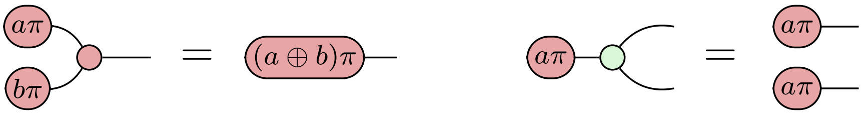

Figure 1.17: X spider as a XOR gate (left) and Z spider as a COPY gate (right).

Let us now consider the natural commutation relation of the classical XOR and COPY gates. It is clear that XORing two bits then copying them is the same as copying the same two bits, then XORing them. Using this relation as motivation, we define the *bialgebra* rule as follows.

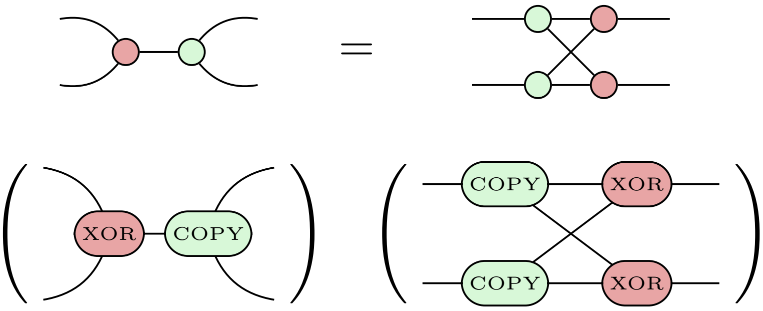

Figure 1.18: The bialgebra rule (top) and its classical motivation (bottom).

The bialgebra rule is then the quantum generalisation of the XOR-COPY commutation relation. It holds for all states, not just the computational basis states.

Hopf Rule

Finally, we have the Hopf rule, which states that we can remove the wires connecting an X spider and a Z spider when the number of connections between them is two. Like with the bialgebra rule (1.2), we can take motivation from the behaviour of the classical XOR and COPY gates, since COPYing two bits then XORing them always yields 0.

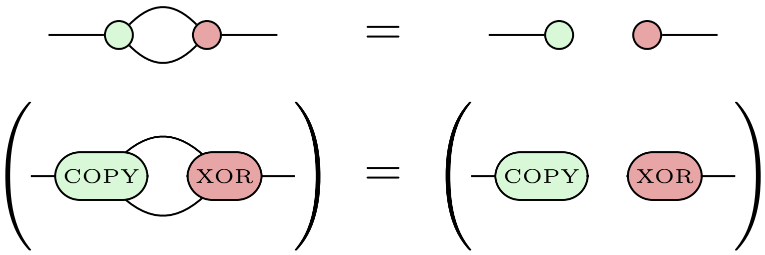

Figure 1.19: The Hopf rule (top) and its classical motivation (bottom).

Chapter 2

Pauli Gadgets

A Pauli string P is defined as a tensor product of the members of the Pauli group $P \in \{I, Y, Z, X\}^{\otimes n}$, where each Pauli operator acts on a distinct qubit (indicated by the subscript). Note that the Pauli matrices are Hermitian operators, and therefore, so are Pauli strings. For convenience, we will drop the subscripts.

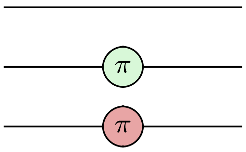

$$= I_0 \; Z_1 \, X_2 = I \otimes Z \otimes X$$

Stone's Theorem [6] states that a strongly continuous one parameter unitary group $U(\theta)$ is generated by a Hermitian operator, P.

$$U(\theta) = e^{i\theta P} = 1 + i\theta P + \frac{1}{2}[i\theta P]^2 + \frac{1}{6}[i\theta P]^3 + \ldots$$

There is therefore a one-to-one correspondence between Hermitian operators and one parameter unitary groups [2]. The time evolution of a quantum mechanical system, described by the Hamiltonian H, is defined by the one parameter unitary group e^{itH}, whilst arbitrary rotation gates in the Z, X and Y bases are described by the one parameter unitary groups of the Pauli matrices Z, X and Y.

$$R_Z(\theta) = e^{i\frac{\theta}{2}Z} \qquad R_Y(\theta) = e^{i\frac{\theta}{2}Y} \qquad R_X(\theta) = e^{i\frac{\theta}{2}X}$$

Phase gadgets are defied as the one parameter unitary groups of Pauli strings consisting of the I and Z matrices, $P \in \{I, Z\}^{\otimes n}$.

$$\Phi(\theta) = \exp\left[i\frac{\theta}{2}(I \otimes Z \otimes Z \otimes \dots)\right]$$

In quantum circuit notation, phase gadgets are represented by a layer of CNOTs followed by a rotation in the Z basis, followed by another layer of CNOTS.

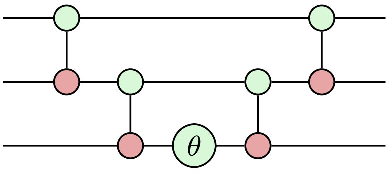

$$= \exp\left(i\frac{\theta}{2} Z \otimes Z \otimes Z\right)$$

The first layer of CNOTs can be thought of as computing the parity of the input qubits by creating an entangled state. The rotation in the Z basis then rotates the entangled state by $e^{i\theta/2}$ or $e^{-i\theta/2}$, depending on its parity. The final layer of CNOTs can be thought of as uncomputing the parity. Since phase gadgets correspond to diagonal unitary matrices in the Z basis, they apply a global phase to a given state without changing the distribution of the observed state [2].

There are many equivalent ways of expressing the same phase gadget in terms of CNOT gates and Z rotation gates. Furthermore, the diagonal action of phase gadgets suggests that a more symmetrical structure exists for phase gadgets in the ZX calculus.

Indeed, we find that by iteratively applying the bialgebra rule, we can represent phase gadgets as follows.

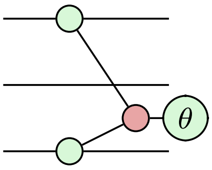

$$= \exp\left(i\frac{\theta}{2} Z \otimes I \otimes Z\right)$$

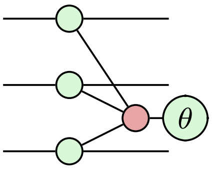

$$= \exp\left(i\frac{\theta}{2} Z \otimes Z \otimes Z\right)$$

By deforming our diagram d and using the spider fusion f (1.2), identity id (1.2) and bialgebra ba (1.2) rules, we are able to show the correspondence between phase gadgets in normal quantum circuit form and in their form in the ZX calculus.

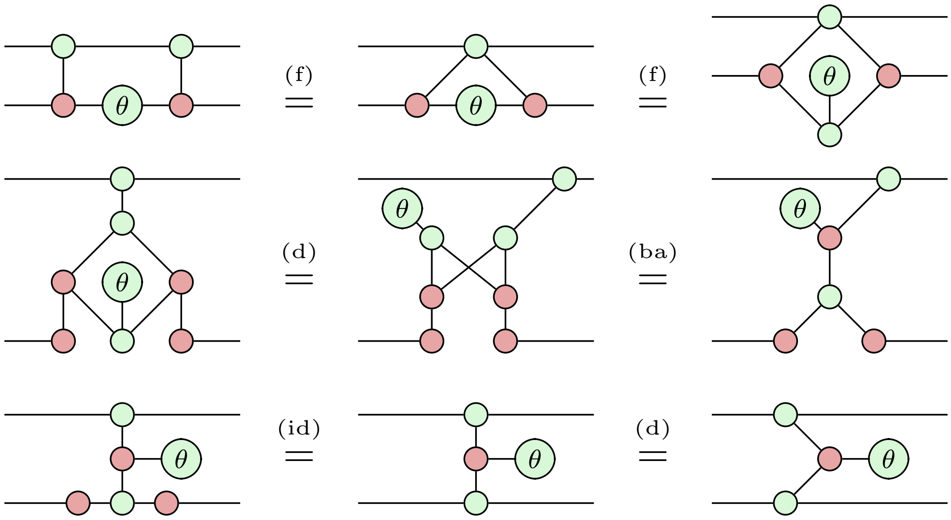

It is then a simple matter of recursively applying this proof to phase gadgets in quantum circuit form to generalise it to arbitrary arity phase gadgets.

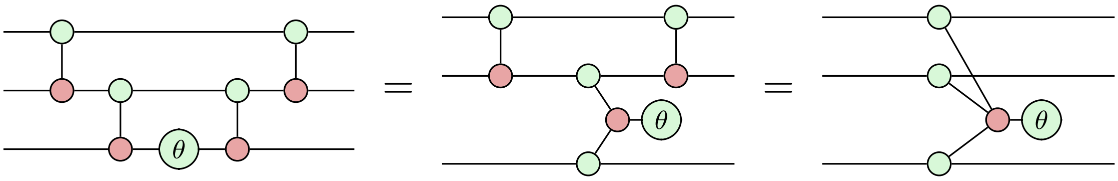

2.1 Phase Gadgets

1. zx representation
2. algebraic structure
3. relation to chemistry
4. phase gadget decomposition / ladder / bricklayering

2.2 Pauli Gadgets

$$C \in \text{Clifford} \qquad P \in \text{Pauli}$$

$$\text{prove: } Ce^{P}C^{\dagger} = e^{CPC^{\dagger}}$$

$$CP^{n}C^{\dagger} = (CPC^{\dagger})^{n}$$

$$Ce^{P}C^{\dagger} = C\sum_{n=0}^{\infty}\left(\frac{P^{n}}{n!}\right)C^{\dagger} = \sum_{n=0}^{\infty}\frac{CP^{n}C^{\dagger}}{n!} = \sum_{n=0}^{\infty}\frac{(CPC^{\dagger})^{n}}{n!}$$

2.3 Commutation Relations

Appendices

Bibliography

[1] Burton, H. G. A., Marti-Dafcik, D., Tew, D. P. & Wales, D. J. Exact electronic states with shallow quantum circuits from global optimisation. *npj Quantum Information* **9** (2023).

[2] Yeung, R. Diagrammatic design and study of ansätze for quantum machine learning (2020). `2011.11073`.

[3] McClean, J. R., Romero, J., Babbush, R. & Aspuru-Guzik, A. The theory of variational hybrid quantum-classical algorithms. *New Journal of Physics* **18**, 023023 (2016).

[4] Kirby, W. M. & Love, P. J. Variational quantum eigensolvers for sparse hamiltonians. *Phys. Rev. Lett. 127, 110503 (2021)* **127**, 110503 (2020). `2012.07171`.

[5] van de Wetering, J. Zx-calculus for the working quantum computer scientist (2020). `2012.13966`.

[6] Stone, M. H. On one-parameter unitary groups in hilbert space. *The Annals of Mathematics* **33**, 643 (1932).